Optics Letters

Coherent control of acoustic phonons by seeded Brillouin scattering in polarization-maintaining fibers

Yaming Feng,[1] Fangxing Zhang,[2] Yuanlin Zheng,[1] Lei Chen,[1] Dongyi Shen,[1] Wei Liu,[1] and Wenjie Wan[1,2,*]

[1]State Key Laboratory of Advanced Optical Communication Systems and Networks, MOE Key Laboratory for Laser Plasmas and Collaborative Innovation Center of IFSA, School of Physics and Astronomy, Shanghai Jiao Tong University, Shanghai 200240, China
[2]University of Michigan-Shanghai Jiao Tong University Joint Institute, Shanghai Jiao Tong University, Shanghai 200240, China
*Corresponding author: wenjie.wan@sjtu.edu.cn

Received 11 October 2018; revised 30 March 2019; accepted 1 April 2019; posted 4 April 2019 (Doc. ID 347479); published 24 April 2019

Coherent excitation of phonons by optical waves, one of the most important channels for light-matter interactions, provides a promising route for optical manipulation of microscopic acoustic phonons for quantum opto-mechanic and phononic devices. Prior research, such as stimulated Brillouin scattering (SBS) in fibers, mainly emphasized phonon amplitude modulation; however, coherent phase control of these phonons has not yet been well explored. Here we experimentally demonstrate a new mechanism to coherently control acoustic phonon phases by a seeded SBS scheme in an optical fiber. Interference between acoustic phonons enables either nearly total transmission or enhanced reflection of optical waves, effectively controlled by phase modulation. This new technique addresses the crucial problem of phase-controlled phonon generation, paving the way for important applications in quantum opto-mechanic and phononic devices.

https://doi.org/10.1364/OL.44.002270

Phonons and collective excitations linking electrons, photons, and heat, play a major role in condensed matter physics affecting many important properties such as thermal conductivity, electrical conductivity, and electron spins [1,2]. The ability to coherently control both the amplitudes and phases of these vibrating atomic chains lies at the heart of various promising technologies ranging from photochemistry, ultrafast science, and thermal physics [3,4]. Coherent excitations of phonons mainly rely on electrical and optical means [5,6], for example, in a pump-probe scheme [7]. However, coherent control of phonons, especially their phases, remains a big challenge. Previously, a multi-pulse pump-probe scheme has been implemented to enhance or suppress coherent phonons through their phase relations by adjusting the delays between the pump laser pulses [8]. In a photonic fiber, the acoustic phonons can be coherently controlled by the sequences of the laser pulses. The preferred acoustic resonance could be enhanced or attenuated by adjusting the delay between the pulses [9]. It becomes even more challenging for such photon-phonon interactions in a low power regime. Under this circumstance, both photon and phonon cavities have to be simultaneously constructed to enhance the insides of the optical and acoustic fields for encouraging photon-phonon interactions [10]. For example, a distributed Bragg reflector type of phonon cavity can be grown with alternating layer of super-lattices to trap both phonon and photon simultaneously [11]; light can also be nonlinearly scattered by stimulated Brillouin scattering (SBS) inside an opto-mechanics cavity [12]. All of these prior studies open up a new opportunity to manipulate phonons through a light fashion. Even for a basic optical waveguide structure such as a fiber, the SBS process can also manifest itself to bridge the optical and acoustic waves. On one hand, this creates an inevitable problem for transmitting large power optical signals, which traditionally can be solved by a pump modulation method [13], fiber structure design [14], and polarization control [15]. On the other hand, such a waveguide structure can be regarded as a unique platform to investigate phonon-photon interactions aiming to coherently control acoustic phonons in an optical way.

In this Letter, we experimentally demonstrate a coherent controlling method of acoustic phonons through a seeded SBS process in a polarization-maintaining fiber (PMF). Two groups of acoustic phonons are individually excited by two pairs of pump-probe optical waves along the fast and slow axes of a PMF, separately, so that these acoustic phonons coincide with the same frequency under rigid phase-matching conditions defined by the birefringence of the two axes. In this manner, we obtain the access to coherently control each phonon's phase by modulating the corresponding pump-probe pair's relative phase delay, which further enables constructive enhancement or destructive suppression of phonons through interference. As a result, we can almost totally eliminate the effect of SBS for one optical mode, allowing SBS-free propagation of optical waves. We believe this new coherent control of phonons may pave the way to a new level of phonon-photon interactions for on-chip phononic applications and phase-sensitive processes in quantum devices.

Momentum conservation plays an important role in the fiber SBS process, effectively determining the backward Stokes

wave's central frequency with respect to its forward signal beam's through a rigid phase-matching condition [16]. Under this frame, the individual phases of optical Stokes waves and acoustic waves, however, are in a random fashion, given that the nature of the SBS wave arising from a randomized background quantum fluctuation [17]. Solely varying the pump wave's phase will not directly alter the acoustic wave's phase, unless the backward Stokes wave has a well-defined phase. Previously, a seeded SBS scheme is achieved in a way called Brillouin dynamic grating (BDG) formed by a pump-probe pair structure where a secondary probe beam is launched oppositely to lock the backward Stokes wave in the frequency domain. This method was explored to enhance SBS processes for sensing purposes in both optical fibers and on-chip waveguides [18]. However, one important aspect of phase controlling has not yet been studied. Here we would like to explore this unique setup for manipulating an acoustic phonon phase through optical waves.

Figure 1(a) shows the basic working principle of the phase-controlling mechanism in SBS processes: a continuous-wave pump laser and a backward probe laser with a frequency offset of Brillouin frequency are paired to form a BDG which is in-phase with the forward propagating longitudinal acoustic phonon induced through the electrostriction effect [19]. In such a manner, the acoustic phonon's phase can be actively controlled by the relative phase between the pump and probe lights. After that, this phase variation of acoustic phonon can be sensed by interfering with a second phonon induced by a second pump-probe pair, as shown in Fig. 1(c). For example, in a PMF, a small birefringence index difference between the fast and the slow axes introduces a small frequency shift to both the pump and the probe for the same phonon mode, as shown in Fig. 1(b). Based on this unique platform, one can coherently control an individual phonon's phase through a pump-probe pair. Meanwhile, the interference of two acoustic phonons will enhance or suppress the BDGs, which subsequently alters the reflection and the transmission of these pump-probe pairs. Here the acoustic wave in a fiber represented is given as [19,20]

$$\tilde{\rho}(x,y,z,t) = S(x,y)\frac{\varepsilon_0\gamma_e q^2 A_1(z,t)A_2^*(z,t)}{\Omega_B^2 - \Omega^2 + i\Omega\Gamma_B}e^{i(\Omega t - qz + \Phi)} + \text{c.c.}, \tag{1}$$

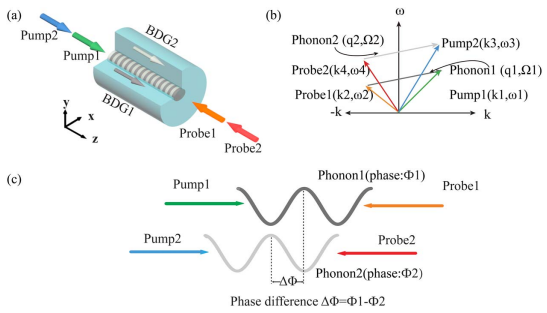

Fig. 1. Schematic of coherently controlling phonons in a PMF. (a) Acoustic Phonon1 is excited by Pump1-Probe1 waves along the slow axis of the PMF. Simultaneously, acoustic Phonon2 is excited by Pump2-Probe2 along the fast axis. (b) Phase-matching conditions for the SBS phonon excitations along the slow and fast axes with different dispersion slopes. (c) Phases of phonons are controlled by pump-probe pairs' phase delays. The two acoustic phonons can interfere with each other regarding their relative phase.

$$S(x,y) = \frac{\langle F_A(x,y)F_O^2(x,y)\rangle F_A(x,y)}{\langle F_A^2(x,y)\rangle}, \tag{2}$$

where $F_A(x,y)$ and $F_O(x,y)$ are the spatial distribution of the fundamental acoustic and optical mode profiles in fiber. γ_e, ε_0, Γ_B, and Ω_B are the electrostrictive constant, vacuum permittivity, Brillouin linewidth, and Brillouin frequency, respectively. $\Omega = \omega_1 - \omega_2$, $q = 2\kappa_1$, and $\Phi = \varphi_1 - \varphi_2$ are the frequency, wave vector, and initial phase of the acoustic wave, respectively, where $\omega_{1,2}$, $\kappa_{1,2}$, and $\varphi_{1,2}$ are the angular frequency, wave vector, and initial phase of the pump and probe lights, respectively. Obviously, the acoustic phonon's phase Φ can be easily regulated by modulating either the pump or the probe's phases under the phase-matching condition, i.e., $\Omega = \omega_1 - \omega_2$ and $q = 2\kappa_1$, strictly requiring both energy and momentum conservations [19]. Note that dispersion or birefringence effects also play an important role in this phase-matching scheme through wave vectors $\kappa_{1,2}$. In a PMF, the index contrast of fast and slow axes $\Delta n = n_x - n_y$ induces a frequency shift of the pumps for SBSs, accordingly [21]:

$$\Delta\omega = \Delta n\frac{\omega_1}{n_y}. \tag{3}$$

This creates a unique scheme for us to access the same acoustic phonon modes through two different polarization optical modes.

Figure 2(a) shows a schematic diagram of the experimental setup of a phase-controlled phonon interference effect. Two tunable lasers TL1,2 (NKT, Koheras Boostik E15) with an ultra-narrow linewidth (<0.1 KHz) are used as the light

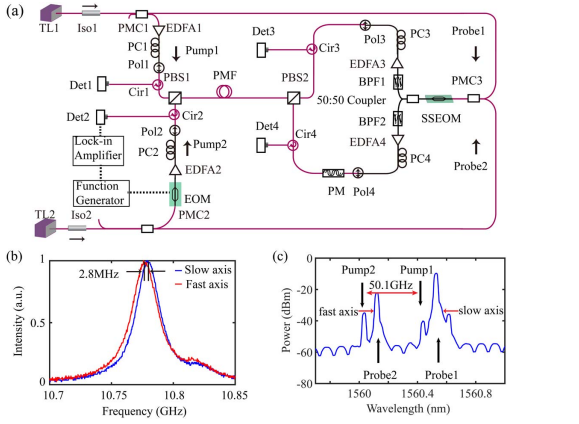

Fig. 2. Experimental scheme of pump-probe seeded SBS processes in a PMF. (a) Experimental setup for coherent control of acoustic phonons in a PMF. The red and black lines represent PMFs and SMFs, respectively. (b) BGSs of the two axes in the PMF. The difference between the central frequencies of the two BGSs is about 2.8 MHz caused by the birefringence of the PMF. (c) Reflected spectrum of the four waves measured by an optical spectrum analyzer (OSA). The frequency differences of the two pump-probe pairs are 10.7805 GHz. Pump1 is set at 1560.5000 nm, and Pump2 is about 1560.0928 nm, which is upshifted by 50.1 GHz according to Eq. (3). TL1,2, 1560 nm tunable laser; Iso1,2, isolator; PMC1,2,3, polarization-maintaining coupler; PM, phase modulator; PC1,2,3,4, polarization controller; Pol1,2,3,4, polarizer; EDFA1,2,3,4, Er-doped fiber amplifier; Cir1,2,3,4, circulator; Det1,2,3,4, InGaAs biased detector; PBS1,2, polarization beam splitter; PMF, polarization-maintaining fiber; SSEOM, single-sideband electro-optical modulator; BF1,2, bandpass filter.

sources. The laser TL1 whose wavelength centers at 1560.5 nm is divided equally by a 3 dB polarization-maintaining coupler (PMC1): one arm is amplified by EDFA1 to serve as Pump1, while the other arm is frequency-downshifted by the Brillouin frequency 10.7805 GHz along the slow axis by a single-sideband electro-optical modulator (SSEOM) to serve as Probe1. This pump-probe pair is launched into the slow axis of a 60 m long PMF (Fujikura, 1550 nm PANDA fiber), together from opposite sides by PBS1 and PBS2. SBS amplification occurs easily in this configuration, even if the power of the Probe1 is relatively small (<1 mW). A second pump-probe pair is constructed through a similar setup from a TL2; however, they are launched into the fast axis of the PM fiber. Several narrow bandpass filters and EDFAs are placed, accordingly, in each path to assist monitoring of the transmission and the reflection signals for optical waves. Figure 2(b) shows the Brillouin gain spectra (BGSs) of the slow (blue) and fast (red) axis scanning the probe when both pump lights' wavelengths center at 1560.5000 nm, and the spectrum bandwidth reads around 23.6 MHz, inversely proportional to the phonon lifetime. The measured central frequency difference of the two BGSs is $\Delta f_{\mathrm{BGS}} = 2.8094$ MHz, giving that the refractive index difference $\Delta n/n_y$ between the two axes is about 2.6060×10^{-4} obtained by [21]

$$\frac{\Delta n}{n_y} = \frac{\Delta f_{\mathrm{BGS}}}{f_{\mathrm{slow}}}, \tag{4}$$

where $f_{\mathrm{slow}} = 10.7805$ GHz is the central frequency of the BGS along the slow axis, and $n_y = 1.4632$. Hence, the wavelength of Pump2 can be determined as 1560.0923 nm through Eq. (3), i.e., $\Delta\omega/2\pi = 50.10$ GHz blueshifted from the Pump1, to access the same phonon mode at 10.7805 GHz along the fast axis in Fig. 2(c).

The optical fiber can support both optical and acoustic modes, as shown in Fig. 3, the fundamental mode profiles of photons in Figs. 3(d) and 3(e) in the slow and fast axes and longitudinal acoustic phonons mode LP_{01} in Fig. 3(b)

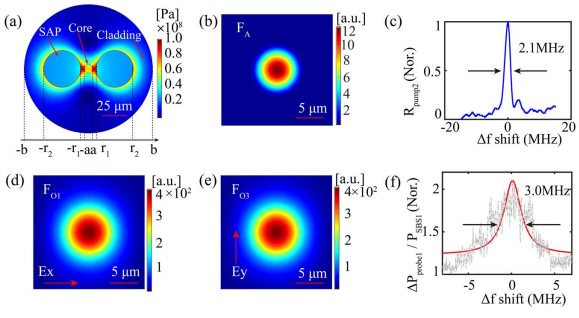

Fig. 3. Birefringence of the PMF is the result of the von Mises stress shown in (a). The radii of the core, the stress-applying parts (SAPs), and the cladding are $a = 4.2$ μm, $(r_2 - r_1)/2 = 18$ μm, and $b = 62.5$ μm, respectively. The distance between the SAPs is 51.4 μm. As a result, the optical modes could be coupled in the (d) slow axis or (e) fast axis, with the electrical field's polarization along the x or y directions, respectively. However, unlike the optical mode, only the longitudinal acoustic mode LP_{01} could be excited, as shown in (b). Linewidth of the BDG is about 2.1 MHz, seen in (c). Interaction linewidth of the two BDGs is about 3.0 MHz, by measuring the normalized power variation of Probe1 $\Delta P_{\mathrm{Probe1}}/P_{\mathrm{SBS1}}$. Gray dashed line, experimental data; red solid line, fitting curve.

can be calculated numerically through the finite element method under a stress distribution, as shown in Fig. 3(a), which is also calculated using a similar method as in the Ref. [22] for a Fujikura PANDA PMF. Note that such induced stress can affect both the polarization properties for photon modes and acoustic modes due to a stress-induced velocity change [22]. The mode profiles for optical modes, including both pump and probe lights on both axes, have similar effective diameters of 10.4 μm, given their small difference in refractive indexes. Meanwhile, the acoustic mode is more tightly confined with the effective diameter around 8.2 μm. Under this circumstance, we first experimentally examine the linewidth of the BDG formed by pump-probe pair1 to be around 2.1 MHz, as shown in Fig. 2(c), obtained by measuring the reflectance of Pump2: R_{Pump2} (without Probe2) when scanning the frequency of Pump2 in the slow axis. This linewidth is reversely proportional to the length of interaction regime, i.e., the 60 m long PM fiber, reflecting the finite length effect of any optical grating structure [21]. Furthermore, when the BDG2 is also present, the FWHM of this interaction between the two BDGs is about 3.0 MHz, as shown in Fig. 3(f), which is the same order as the linewidth of BDG. This is obtained by measuring the normalized changing power of Probe1: $\Delta P_{\mathrm{Probe1}}/P_{\mathrm{SBS1}}$ with scanning the whole pump-probe pair2's central frequencies while keeping their phase difference as a constant, where P_{SBS1} is the increased power of Probe1 by the SBS process in the slow axis (SBS1) without BDG2. Here the power of Pump1-Probe1, Pump2-Probe2 optical waves are set at 60, 5, 70, and 50 mW, respectively. With this configuration, we are ready to explore the phase controlling mechanism in the next step.

Figure 4 demonstrates both the coherent phase and power control of phonons during seeded SBS processes. As mentioned above, the individual phonon's phase can be regulated by the pump-probe's relative phase. In order to control the phase difference between the two phonons, $\Delta\Phi = \varphi_{12} - \varphi_{34}$, a phase

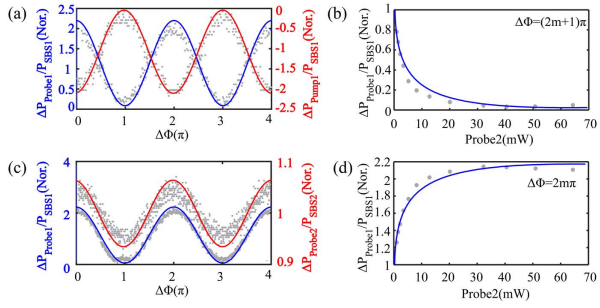

Fig. 4. Coherent control of acoustic phonons: the experimental (gray circular dot) and numerical simulation results (solid line). (a) Normalized power variations of Probe1: $\Delta P_{\mathrm{Probe1}}/P_{\mathrm{SBS1}}$ (blue solid line) and Pump1: $\Delta P_{\mathrm{Pump1}}/P_{\mathrm{SBS1}}$ (red solid line) periodically vary when modulating $\Delta\Phi$ in a range of 4π. These two curves are synchronous, but out of phase. Meanwhile, the normalized power change of Probe2: $\Delta P_{\mathrm{Probe2}}/P_{\mathrm{SBS2}}$ varies synchronously in phase with $\Delta P_{\mathrm{Probe1}}/P_{\mathrm{SBS1}}$ shown in (c). These transmission or reflection changes directly indicate the fact that the two phonons are constructively enhanced or destructively annihilated through their interference. The powers of the two pump-probe light pairs are 60, 5, 70, and 50 mW. (b) and (d) show that $\Delta P_{\mathrm{Probe1}}/P_{\mathrm{SBS1}}$ varies while increasing Probe2 linearly from 0 to 65 mW with $\Delta\Phi = (2m+1)\pi$, and $\Delta\Phi = 2m\pi$, $m = 1, 2, 3, \ldots$, separately. The powers of Pump1, Probe1 and Pump2 are still fixed at 60, 5, and 70 mW, respectively.

modulator is used in the Probe2 path to control φ_{34} and, further, to change $\Delta\Phi$, as shown in Fig. 2(a). As a result, the peak positions of phonon 2 would move relatively to the other phonon through varying the phase $\Delta\Phi$, effectively leading to the interference between the two phonons. In the meantime, by measuring the power variation of Probe1 and Pump1, $\Delta P_{\text{probe1}}/P_{\text{SBS1}}$ and $\Delta P_{\text{pump1}}/P_{\text{SBS1}}$ simultaneously, we observe energy oscillation between the forward pump and the backward probe beams with respect to this phase varying in Fig. 4(a). Both the values of $\Delta P_{\text{probe1}}/P_{\text{SBS1}}$ and $\Delta P_{\text{pump1}}/P_{\text{SBS1}}$ vary sinusoidally, however, out of phase to each other. Meanwhile, the sum of $\Delta P_{\text{probe1}}/P_{\text{SBS1}}$ and $\Delta P_{\text{pump1}}/P_{\text{SBS1}}$ remains zero all the time due to the energy conservation in the slow axis. This shows the most important fact that phonons inside the fiber have been coherently enhanced or suppressed by such phase control. Another strong evidence for this conclusion comes from the measurement of the power change of Probe2: $\Delta P_{\text{probe2}}/P_{\text{SBS2}}$ in the fast axis, which oscillates synchronously in-phase with $\Delta P_{\text{probe1}}/P_{\text{SBS1}}$, where P_{SBS2} is the increased power of Probe2 by SBS in the fast axis (SBS2) without BDG1. This proves that the same phonon mode is experiencing such interfering enhancement or suppression along the fast axis as well, as shown in Fig. 4(c).

In addition, the acoustic phonon amplitudes are determined by the product of both pump-probe pairs, seen from Eq. (1). Hence, for a given phase delay between two phonons, one can also control the phonon's amplitude by varying the power of one of probes power either to enhance or suppress the acoustic phonon. Figures 4(b) and 4(d) show $\Delta P_{\text{Probe1}}/P_{\text{SBS1}}$ varying with respect to Probe2's power increment at two representative phase delays: destructive and constructive ones. For the phonon suppression case, as shown in see Fig. 4(b), i.e., $\Delta\Phi = 2m\pi$, $m = 1, 2, 3\ldots$, Probe1's power drops quickly from 21.5 to 6.9 mW when increasing Probe2 from 0 to 12 mW. Further increasing Probe2 till 50 mW, Probe1 gradually decreases to its minimum around 5.5 mW, only amplified by 0.5 mW through SBS. In the meantime, Pump1's transmission reaches near unit. In another words, we can achieve an almost SBS-free situation for pump-probe1's propagation by suppressing the phonons. After that, saturation effects dominate, and no further phonon suppression occurs. Here the reason for this saturation effect is due to the strong depletion of Pump2 while increasing P_{Probe2}; as a result, the phonons would not grow linearly anymore, and similar effects have also been observed in a photonic chip previously [23]. For the phonon enhancement, the exact opposite phenomenon occurs, also accompanied by the saturation effect, as shown in Fig. 4(d).

In conclusion, coherent phase-controlled acoustic phonons can be generated in a seeded SBS in an optical fiber. Optically phase-controlled phonons interfere constructively or destructively to prohibit or enhance optical transmissions. One SBS-free optical transmission can be achieved by totally suppressing phonons. The new coherent optically control of phonons reported here may open new realms of many applications in quantum, photonic, and phononic devices in the near future.

Funding. National Key Research and Development Program (2017YFA0303700, 2016YFA0302500); National Natural Science Foundation of China (NSFC) (11674228, 11304201, 61475100).

REFERENCES

1. I. Ponomareva, D. Srivastava, and M. Menon, Nano Lett. **7**, 1155 (2007).
2. R. A. Jishi, M. S. Dresselhaus, and G. Dresselhaus, Phys. Rev. B **48**, 11385 (1993).
3. T. Kampfrath, L. Perfetti, F. Schapper, C. Frischkorn, and M. Wolf, Phys. Rev. Lett. **95**, 187403 (2005).
4. Y. Cai, J. Lan, G. Zhang, and Y. W. Zhang, Phys. Rev. B **89**, 035438 (2014).
5. Y. Feng, Y. Zheng, and J. Cao, J. Opt. Soc. Am. B **33**, 105 (2016).
6. K. P. Cheung and D. H. Auston, Phys. Rev. Lett. **55**, 2152 (1985).
7. M. Hase, K. Mizoguchi, H. Harima, S. I. Nakashima, and K. Sakai, Phys. Rev. B **58**, 5448 (1998).
8. D. H. Hurley, R. Lewis, O. B. Wright, and O. Matsuda, Appl. Phys. Lett. **93**, 113101 (2008).
9. G. S. Wiederhecker, A. Brenn, H. L. Fragnito, and P. St. J. Russell, Phys. Rev. Lett. **100**, 203903 (2008).
10. E. Gavartin, R. Braive, I. Sagnes, O. Arcizet, A. Beveratos, T. J. Kippenberg, and I. Robert-Philip, Phys. Rev. Lett. **106**, 203902 (2011).
11. M. Trigo, A. Bruchhausen, A. Fainstein, B. Jusserand, and V. Thierry-Mieg, Phys. Rev. Lett. **89**, 227402 (2002).
12. A. B. Matsko, A. A. Savchenkov, V. S. Ilchenko, D. Seidel, and L. Maleki, Phys. Rev. Lett. **103**, 257403 (2009).
13. M. Tsubokawa, S. Seikai, T. Nakashima, and N. Shibata, Electron. Lett. **22**, 473 (1986).
14. N. Yoshizawa and T. Imai, J. Lightwave Technol. **11**, 1518 (1993).
15. M. M. Howerton, W. K. Burns, and G. K. Gopalakrishnan, J. Lightwave Technol. **14**, 417 (1996).
16. E. P. Ippen and R. H. Stolen, Appl. Phys. Lett. **21**, 539 (1972).
17. R. W. Boyd, K. Rzążewski, and P. Narum, Phys. Rev. A **42**, 5514 (1990).
18. R. Pant, E. Li, C. G. Poulton, D. Y. Choi, S. Madden, B. Luther-Davies, and B. J. Eggleton, Opt. Lett. **38**, 305 (2013).
19. R. W. Boyd, *Nonlinear Optics*, 3rd ed. (Elsevier, 2003), pp. 436–446.
20. G. P. Agrawal, *Nonlinear Fiber Optics*, 5th ed. (Elsevier, 2013), pp. 354–358.
21. K. Y. Song and H. J. Yoon, Opt. Lett. **35**, 2958 (2010).
22. W. Zou, Z. He, and K. Hotate, IEEE Photonics Technol. Lett. **18**, 2487 (2006).
23. B. J. Eggleton, C. G. Poulton, and R. Pant, Adv. Opt. Photonics **5**, 536 (2013).